Molecular-Level Composition and Acute Toxicity of Photosolubilized Petrogenic Carbon

Phoebe Zito,[*,†,‡] David C. Podgorski,[†,‡] Joshua Johnson,[§,∥] Huan Chen,[⊥] Ryan P. Rodgers,[⊥] François Guillemette,[#] Anne M. Kellerman,[∇] Robert G. M. Spencer,[⊥,∇] and Matthew A. Tarr[†]

[†]Department of Chemistry and [‡]Pontchartrain Institute for Environmental Sciences, University of New Orleans, 2000 Lakeshore Drive New Orleans, Louisiana 70148, United States

[§]Department of Natural Sciences, Gardner-Webb University, 110 South Main Street, Boiling Springs, North Carolina 28017, United States

[⊥]National High Magnetic Field Laboratory, Florida State University, 1800 East Paul Dirac Drive, Tallahassee, Florida 32310-4005, United States

[#]Research Center for Watershed Aquatic Ecosystem Interactions (RIVE), Department of Environmental Sciences, Université du Québec à Trois-Rivières, Trois-Rivières, Québec G8Z 4M3 Canada

[∇]Department of Earth, Ocean and Atmospheric Science, Florida State University, 600 West College Avenue, Tallahassee, Florida 32306-4520, United States

Ⓢ *Supporting Information*

ABSTRACT: To examine the molecular-level composition and acute toxicity per unit carbon of the petroleum-derived dissolved organic matter (DOM_{HC}) produced via photo-oxidation, heavy and light oils were irradiated over seawater with simulated sunlight. Increases in dissolved organic carbon concentrations as a function of time were associated with changes in the DOM_{HC} composition and acute toxicity per unit carbon. Parallel factor analysis showed that the fluorescent dissolved organic matter (FDOM) composition produced from the heavy oil became more blue-shifted over time, while the light oil produced a mixture of blue- and red-shifted components similar to FDOM signatures. Ultrahigh-resolution mass spectrometry reveals that the composition of the DOM_{HC} produced from both heavy and light oils was initially relatively reduced, with low O/C. With time, the composition of the DOM_{HC} produced from the heavy oil shifted to unsaturated, high-oxygen compounds, while that produced from the light oil comprised a range of high O/C aliphatic, unsaturated, and aromatic compounds. Microtox assays suggest that the DOM_{HC} initially produced is the most toxic (62% inhibition); however, after 24 h, a rapid decrease in toxicity decreased linearly to 0% inhibition for the heavy DOM_{HC} and 12% inhibition for the light DOM_{HC} at extended exposure periods.

LIGHT EXPOSURE
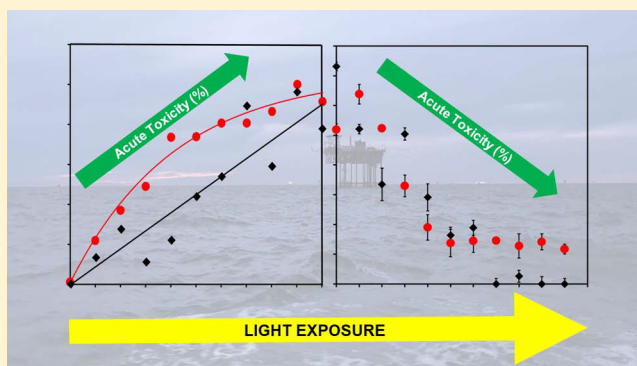
1. INTRODUCTION

Oil spills are a large contributor of petroleum to the ocean and have long-term effects on the surrounding ecosystem as a result of the amount of oil released in one concentrated area. Some of the most notable oil spills to date in the U.S. are the 1989 Exxon Valdez spill, the 2007 Cosco Busan oil spill, and the 2010 Deepwater Horizon (DWH) oil spill. The most publicized and researched spill, the DWH, released about 200 000 metric tonnes over a period of 86 days. Of that, an estimated $9 \pm 4 \times 10^7$ kg of hydrocarbons formed slicks at the surface of the Gulf of Mexico post spill.[1−3] Although the DWH oil spill occurred almost a decade ago, there are still unanswered questions regarding the fate of the oil. Publications in 2017 and 2018 from the Sea Grant Oil Spill Outreach Program discuss the many different routes and processes of oil removal but state that there is still 11−25% of the oil remaining unaccounted for in the environment.[4]

Once petroleum enters the environment, it can undergo many chemical and physical changes. As a result of its dark color, it is optically active (contains many chromophores) and can undergo photodegradation, which is an important degradation process in the environment.[5−7] These photodegradation processes result in the formation of oxyhydrocarbons, a term used to describe petroleum compounds that are formed upon degradation by the oxygenation of hydrocarbons.[8] Some oxyhydrocarbons are polar enough to

dissolve into water, becoming highly mobile and bioavailable in the ecosystem.[9] There have been numerous published studies for dissolved organic matter (DOM) produced in water that was in contact with petroleum collected from field samples[10−12] or in laboratory experiments.[9,13−15] Both provide evidence that petroleum is a viable source of carbon for production of petroleum-derived DOM (DOM$_{HC}$) upon photooxidation. However, these previous studies did not investigate how the molecular composition, optical properties, dissolved organic carbon (DOC) concentrations, and toxicity of DOM$_{HC}$ change as a function of sunlight exposure.

This study investigated the quantity of DOC and quality of DOM compounds that are produced when thin oil films were subjected to sunlight over time as well as their potential toxicity. The objectives for this study were to (1) quantify the amount of DOC produced from thin oil films over extended irradiation times, (2) examine changes in optical properties of DOM$_{HC}$, (3) characterize DOM$_{HC}$ at the molecular level to determine changes in composition occurring at each exposure time period, and (4) examine relationships between acute toxicity per unit carbon and the chemical composition of DOM$_{HC}$ as a function of exposure time. There is a general paucity of laboratory studies surrounding the characterization, transformation, and toxicity of DOM$_{HC}$ produced from the photodissolution of petroleum. Identifying the optical and molecular composition of DOM$_{HC}$ and how it changes over time can lead to important inferences about how it influences bioavailability, dissolution, and toxicity in the environment.

2. MATERIALS AND METHODS

2.1. Samples and Reagents. The oils used in this study were NIST 1621e heavy fuel oil (nist.gov) and a surrogate Macondo oil (MC) (provided by BP August 2011, chain of custody number 20110803-Tarr-072). From herein, 1621e and MC are referred to as heavy and light oils, respectively. Seawater collected from the Gulf of Mexico by the Louisiana Universities Marine Consortium (LUMCON) (35 ppt salinity, pH 8.3, and DOC of 1.5 ppm) was previously filtered through precombusted (450 °C, >5 h) 0.27 μm glass microfiber filters (Advantec). All glassware was acid-cleaned and combusted at 550 °C prior to use. Nanopure water was collected from an Aeries nanopure system. All reagents were high-performance liquid chromatography (HPLC)-grade and purchased from JT Baker.

2.2. Photoproduction of DOM$_{HC}$. Thin oil films of 120 μm[16] were created with 388 mg of heavy oil and 325 mg of light oil and spread over 50 mL of seawater. To decrease viscosity and create even films across the surface of the water, the heavy oil was mixed with 100 μL of toluene and 2 mL of pentane prior to pouring it over the seawater. Both solvents were evaporated for 10 min in a fume hood before incubation experiments. The oil films were then incubated in a solar simulator (Atlas Suntest CPS+, Atlas Material Testing Technology LLC) set at 765 W/m^2, which was equivalent to 4 days of natural sunlight in the Gulf of Mexico per 24 h interval.[17−19] Each individual jacketed beaker, thermostatically controlled at 27 °C, was representative of a single time period from 0 to 240 h (exposures were performed in batches of two beakers at a time). Quartz lids were securely placed on top of each beaker to reduce evaporation yet allow the light to transmit to the oil films. A dark control (no light exposure) for each oil was incubated for 240 h and denoted as T$_{0 h}$. This sample is $T = 0$ in all figures and data interpretation. After

exposure, the water was collected and filtered through 0.27 μm glass microfiber filters and stored at 4 °C until analysis.

2.3. DOC and Excitation−Emission Matrix (EEM) Spectroscopy Measurements. DOC concentrations were measured with a Shimadzu total organic carbon (TOC) analyzer using a high-temperature combustion method and a platinized alumina catalyst. Each sample was diluted 1:3 (v/v) with nanopure water acidified to pH 2 using 12 M HCl. The sample concentrations were determined using a five-point calibration curve between 0 and 50 ppm of potassium hydrogen phthalate (KHP). Blank injections were run in-between each sample injection, and bracketing standards were run every 10 sample injections and at the end of the analyses. To ensure the samples were within the calibration curve, the auto dilution feature on the TOC analyzer was enabled. The acidified samples (pH 2) were sparged for 5 min at 75 mL/min with ultrapure air to remove inorganic carbon from samples prior to the measurement. The mean of three to five injections of 25 μL is reported for every sample, and the coefficient of variance (CV) was <2% for replicate injections. DOM samples were analyzed using EEM fluorescence spectra measured on a Horiba Aqualog fluorimeter. Samples were measured in a 10 mm quartz cell at a constant room temperature of 20 °C. Sealed water cell blanks were run prior to analysis to test instrument stability using the Raman peak of water, at excitation of 350 nm and emission of 340−420 nm. Excitation wavelengths ranged from 240 to 800 nm at 5 nm increments, while emission wavelengths were collected every 2 nm from 245 to 800 nm. All samples were dilution-corrected to $A_{254\ nm}$ = 0.1 using nanopure water to overcome inner-filter effects (IFEs).[20,21] Absorbance measurements were performed to confirm that Beer's law was upheld for the DOM$_{HC}$ (concentration ranges from 3.125 to 50 μg/mL). EEM fluorescence intensities were corrected for Rayleigh and Raman scattering, nanopure water blank subtracted, and instrument bias in excitation and emission prior to correction for any remaining IFEs.[22] DOM$_{HC}$ samples were adjusted to pH 8 prior to analysis.[23−25] The humification index (HIX) was calculated by dividing the area under an emission range of 435−480 nm by the sum of the peak area of 300−435 and 435−480 nm, with excitation at 254 nm[20] (Table S1 of the Supporting Information).[23−25] Specific ultraviolet (UV) absorption at 254 nm (SUVA$_{254}$) was calculated for the DOM$_{HC}$ by dividing the decadal absorption coefficient at 254 nm by the DOC concentration (mg of C/L), giving units of L mg^{-1} of C m^{-1} (Table S1 of the Supporting Information).[26]

2.4. Microtox Screening. The DOM$_{HC}$ water samples were assessed for acute toxicity per unit carbon (N = 22; Microtox model 500 analyzer, Modern Water, New Castle, DE, U.S.A.).[27] This *Vibrio fischeri* bioluminescence inhibition assay was selected because its effect concentrations are correlated to other aquatic toxicity end points and it is suitable for toxic equivalency evaluation of complex environmental samples, including groundwater, where it has been shown to correlate well with the *in vivo Daphnia magna* toxicity assays.[28] Filtered light DOM$_{HC}$ water samples were carbon-normalized to 20 ppm of C (dark control was preconcentrated to 10 ppm) with 0.27 μm filtered, autoclave-sterilized 70% artificial seawater (Instant Ocean Aquarium Systems, Inc., Mentor, OH, U.S.A.). The pH of the samples was adjusted to 7, and the samples were transferred to a glass cuvette, enriched with the osmotic adjusting solution (sodium chloride solution that brings salinity of the samples to approximately 2%), and analyzed.

Light loss or gain in the samples relative to a control sample (reagent blank provided by the manufacturer) was calculated. The Microtox 81.9% screening test protocol was followed for the toxicity assessment (Microbics Corporation, Carlsbad, CA, U.S.A.).

2.5. Ultrahigh-Resolution Mass Spectrometry. DOM was collected and preconcentrated by the solid-phase extraction technique described in detail elsewhere.[29] Briefly, each sample was passed through a precombusted 0.27 μm glass-fiber filter and acidified to pH 2 prior to loading onto a Bond Elut PPL (Agilent Technologies) stationary phase cartridge. Each sample was then desalted with pH 2 nanopure water and eluted with methanol at a final concentration of 100 μg of C mL^{-1}. The extracts were stored in the dark at 4 °C in precombusted glass vials until analysis by negative-ion electrospray ionization coupled with a custom-built Fourier transform ion cyclotron resonance mass spectrometer equipped with a 9.4 T superconducting magnet [National High Magnetic Field Laboratory (NHMFL), Florida State University, Tallahassee, FL, U.S.A.).[30−32] Each mass spectrum was internally calibrated with a "walking" calibration equation, followed by molecular formula assignment with EnviroOrg software provided by the NHMFL.[33,34] The MS signals were normalized to the most abundant signal in each spectrum. The modified aromaticity index (AI$_{mod}$) of each formula was calculated, and AI$_{mod}$ values of 0.5−0.67 and >0.67 were classified as aromatic and condensed aromatic structures, respectively.[35] Other compound categories were highly unsaturated (low oxygen), AI$_{mod}$ < 0.5, H/C < 1.5, and O/C < 0.5; highly unsaturated (high oxygen), AI$_{mod}$ < 0.5, H/C < 1.5, and O/C > 0.5; and aliphatic, H/C ≥ 1.5−2.0, O/C ≤ 0.9, and N ≥ 0 (Table S1 of the Supporting Information).[35−38]

2.6. Statistical Analyses. Parallel factor analysis (PARAFAC) was conducted on heavy and light DOM$_{HC}$ samples using the drEEM toolbox[22,39] for MATLAB (Mathworks, Natick, MA, U.S.A.).[22] The number of components was determined by a visual inspection of spectral loadings and split half analysis following Murphy et al.[39] Fluorescence intensities [expressed as Raman units (RU)] for each component and sample were corrected for dilution, and the percent relative contribution of each component to total fluorescence was calculated for each sample and exposure period. Principle components analysis (PCA), multivariate methods, and correlations were conducted using the JMP software, version 13.1.0 (SAS Institute, Cary, NC, U.S.A.). PCA was conducted using the percent relative abundance scores, DOC concentrations, chromophoric dissolved organic matter (CDOM) and fluorescent dissolved organic matter (FDOM) spectral indices (Table S1 of the Supporting Information), and compound class scores from Fourier transform ion cyclotron resolution mass spectrometry (FT-ICR MS) results. Spearman rank correlation coefficients were calculated in Python.[38] Spearman rank correlation coefficients were calculated between the relative abundance of assigned molecular formulas in each sample, exposure period, and acute toxicity per unit carbon.

3. RESULTS AND DISCUSSION

3.1. Photodissolution of Petroleum Produces DOC. Increasing concentrations of DOC as a function of exposure period were observed for both the heavy and light petroleum samples. Carbon concentrations, ranging from 10.4 to 197.8 mg of C L^{-1} for the heavy DOM$_{HC}$ and from 7.2 to 234.2 mg of C L^{-1} for the light DOM$_{HC}$, are presented in Figure 1 and
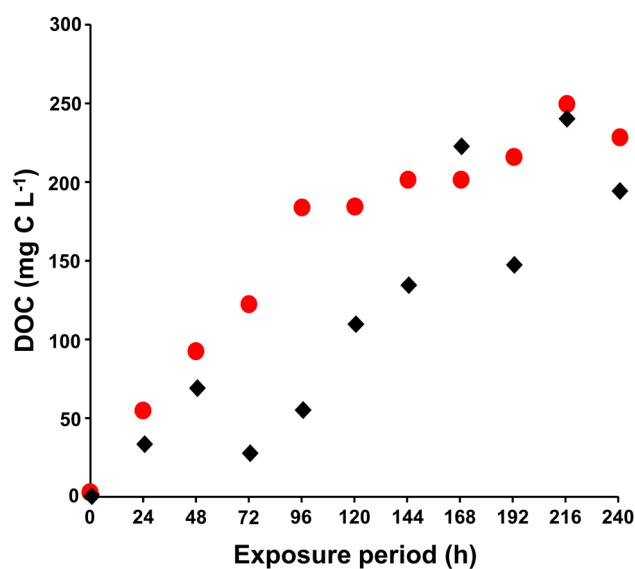
Figure 1. DOC photoproduction for heavy (black diamonds) and light (red circles) DOM$_{HC}$ over time. An increase in the DOC concentration is observed over time with extended light exposure.

Table S1 of the Supporting Information. After an exposure period of 234 h, the DOC concentrations peaked at 242.5 and 255.6 mg of C L^{-1} for the heavy and light DOM$_{HC}$, respectively. Previous studies have also reported elevated DOC concentrations in controlled laboratory settings of water in contact with petroleum after sunlight exposure; however, different amounts of oil and water were used for the incubations, which makes it difficult to directly compare.[13,15] These results show that both the heavy and light petroleum films floating on water can continuously produce DOC under extended photooxidation.

3.2. Optical Properties of DOM$_{HC}$. The use of optical spectroscopy to characterize the CDOM/FDOM in each DOM$_{HC}$ sample provides information regarding the change in composition of the DOM$_{HC}$ over time. Table S1 of the Supporting Information reports the HIX measured in this study at each exposure period for the heavy and light DOM$_{HC}$. The HIX values measured for the heavy and light DOM$_{HC}$ samples increased from 0.33 at T$_{0 h}$ to 2.4 at T$_{240 h}$ and from 0.20 at T$_{0 h}$ to 0.98 at T$_{240 h}$, respectively (Table S1 of the Supporting Information). The overall increase in HIX values after sunlight exposure suggests that both oil films produce DOM$_{HC}$ of increased aromaticity and oxygen content.[20,40,41] Interestingly, when looking at the HIX values relative to each time period, we noticed distinct differences not only between the two DOM$_{HC}$ samples but comparative to each irradiation period. For example, the heavy DOM$_{HC}$ sample exhibited a steady increase in HIX over time, which makes sense considering that the starting composition of the heavy oil is comprised of relatively high molecular weight (MW) and aromatic compounds.[42] Therefore, an increased HIX value would suggest that these higher MW compounds are being oxygenated to the point where they are rendered water-soluble. After the initial production of DOM$_{HC}$ from the light oil, the HIX values stayed relatively constant starting at 1.3 at T$_{24 h}$ to 0.98 at T$_{240 h}$. Maximum SUVA$_{254}$ values were reached at different times for the light DOM$_{HC}$ (from 0.6 L mg^{-1} of C m^{-1} at T$_{0 h}$ to 3.5 L mg^{-1} of C m^{-1} at T$_{48 h}$; Table S1 of the Supporting Information) and heavy DOM$_{HC}$ (from 2.0 L mg^{-1}
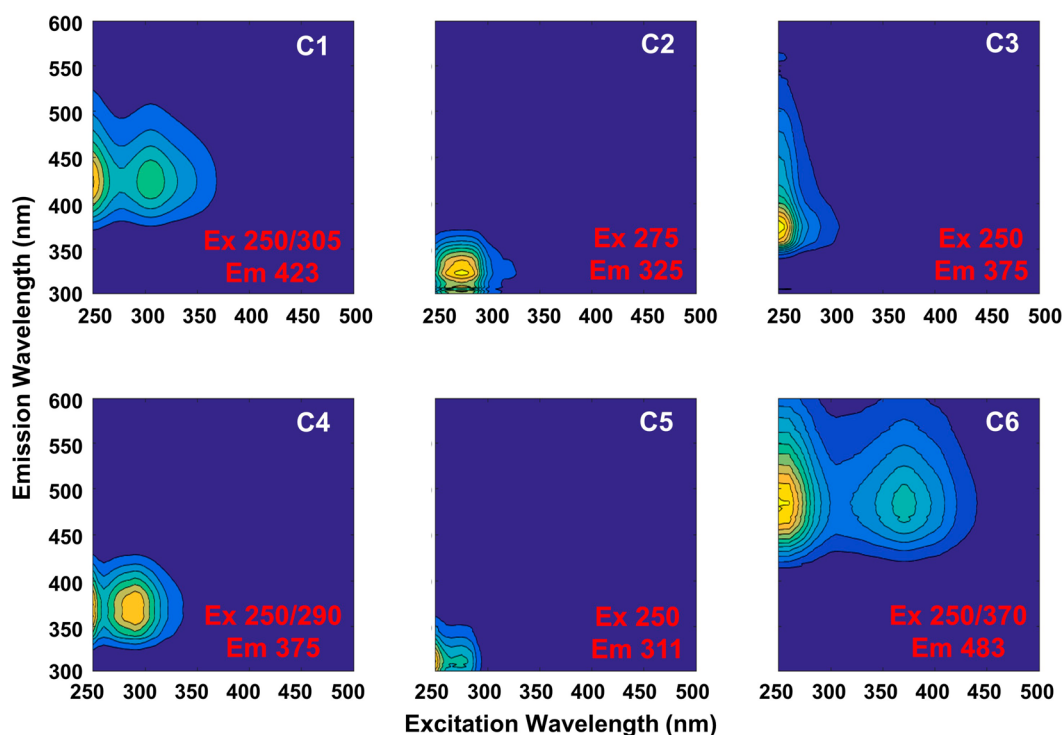
Figure 2. Six-component PARAFAC model constructed from 60 samples for DOM_{HC} produced from heavy and light oils. The maximum excitation and emission are shown in red.

of C m^{-1} at $T_{0 h}$ to 5.5 L mg^{-1} of C m^{-1} at $T_{144 h}$) during the light exposure period. The increase in $SUVA_{254}$ values after initial light exposure signifies that the photodissolution of petroleum produces aromatic DOM_{HC}.[26] The subsequent decrease in $SUVA_{254}$ values over time was not linear, suggesting that the composition of the DOM_{HC} varied over time. This could be due to the production of non-aromatic compounds in DOM_{HC} via indirect photolysis of oil compounds, particularly as DOC increased over time (Figure 1). Furthermore, the heavy DOM_{HC} initially had higher $SUVA_{254}$ values than the light DOM_{HC}, suggesting that the starting composition of the oil affects the composition of DOM_{HC}.

Six fluorescence DOM components were validated from PARAFAC modeling using EEM spectra from 60 DOM_{HC} samples produced from light and heavy oils. Figure 2 shows color contour plots for the six-component PARAFAC model (denoted C1−C6), along with the excitation and emission maxima shown in red. Component 1 (C1) has an excitation peak at 250 nm and a secondary excitation peak at 305 nm, with an emission maximum at 423 nm. Traditionally, this component is described as marine humic-like and corresponds to compounds that are blue-shifted in fluorescence.[43] Components 2 and 5 (C2 and C5) are the most blue-shifted components in this model, with excitation maxima at 275 nm (C2) and 250 nm (C5) and emission maxima at 325 nm (C2) and 311 nm (C5), respectively. These components have been described as tyrosine- and tryptophan-like and comprise the protein-like region of fluorescence.[43,44] Component 3 (C3) red shifts to a longer emission, with an excitation peak at 250 nm and an emission peak at 375 nm. Component 4 (C4) is slightly less blue-shifted than C2 and C5, with an excitation peak at 250 nm, secondary excitation peak at 290 nm, and an emission maximum at 375 nm. Component 6 (C6) is the most red-

shifted component in this study, with an excitation peak at 250 nm, secondary excitation peak at 370 nm, and an emission peak at 483 nm. Component 6 is comprised of fluorophores that have wide excitation bands and long emission wavelengths, which reflect organic matter that contains high MW and aromatic compounds.[45−47] It is important to note that, although these optical components match those mapped for terrestrial and microbially derived DOM, it does not mean that the class of compounds is the same for those components. Furthermore, the oil-derived compounds can match the spectral components without matching the exact structures. Previous studies have shown that singlet oxygen, hydroxyl radical, and organic triplet formation are important pathways when oil and sunlight interact.[48−50] Therefore, we can infer that the longer emission bands in DOM_{HC} produced at longer exposure periods are partially due to the formation of singlet−triplet bands enhanced by the addition of oxygen,[51,52] thus creating "humic" and "fulvic"-like DOM fluorescence signatures.

The model loadings generated from PARAFAC were uploaded into OpenFluor, and a query was conducted to match spectra from our loadings with data from other past studies. After the query was run, there were components from up to 30 PARAFAC models, which had a 0.95 minimum similarity score that matched with four of the six components. C1 and C6 had the most matches from samples collected in oceans, rivers, and lakes.[44,45,53−56] Notably, our C6 matched a study by Gonnelli et al., who analyzed water from an area where high maritime traffic exists and has a high probability for an oil spill.[57] To narrow this number down, we set the minimum similarity score to ≥ 0.98 and found eight hits that matched our PARAFAC components. Included in these eight were databases published by Murphy et al. and Osburn et al., where their C1 and C5 regions matched our C4 and C1,

respectively.[58,59] Both studies characterized our C1 and C4 as terrestrial-derived fluorescence signatures[58,59] that are comparable to the ubiquitous humic-/fulvic-like peaks, suggesting that, as the petroleum compounds become more photodegraded, they produce more red-shifted material and optically resemble the terrestrial-derived material. We know that petroleum does not contain humic and fulvic acids; therefore, these fluorescent signatures are related to molecular-level structure composition and not necessarily source. Components 1, 5, and 6 have DOM-like optical signatures as observed in previously published literature for DOM.[59,60] Component 2 has fluorescence signatures that look similar to the protein-like "T" or "B" peaks traditionally found in terrestrial and marine DOM samples.[60] Component 2 matched with groundwater samples collected from an oil spill that occurred in an underground aquifer.[12] Although we identify fluorescence signatures, peaks T and B, associated with "protein-like" or amino acid fluorescence, these compounds are not present in petroleum. This fact underscores that these fluorescence signatures are indicative of molecular structures and not sources (i.e., microbial, terrestrial, etc.). For example, there were no matches for C3, which suggests a new structural motif not found in non-petroleum-derived DOM that can be used as an indicator component for petroleum-contaminated waters.

Studies have also assessed optical properties of seawater that have been in contact with oil in laboratory studies as well as directly from the Gulf of Mexico post DWH spill.[10,15,61,62] Zhou et al. studied the chemical progression of Macondo crude oil during a laboratory photodegradation study using Teflon bottles and natural sunlight over a period of 105 days.[15] Despite visual similarities, we did not find a match in OpenFluor using a similarity score of >0.95.[10,15,61,62] The lack of matches in OpenFluor may be attributed to the different experimental conditions and analytical preparation used by Zhou et al.[15] For example, no filtering of the samples after the solar incubation was reported; therefore, it is unknown if they were analyzing oil droplets suspended in water or DOM$_{HC}$.

3.3. Molecular-Level Characterization of DOM$_{HC}$. FT-ICR MS was used to characterize the molecular composition of the heavy and light DOM$_{HC}$ time series samples. Figure S1 of the Supporting Information shows trends in the compositional classes measured by FT-ICR MS. These trends are nonlinear with exposure time; therefore, a Spearman rank correlation was used to interpret the data. Figure 3 shows a series of plots using a Spearman rank correlation coefficient for heavy (Figure 3a) and light (Figure 3b) DOM$_{HC}$ with time. The black dotted lines across each plot separate the different classifications of compounds in van Krevelen space for aliphatic, unsaturated, low and high oxygen, aromatic, and condensed aromatic.[36]

The composition of DOM$_{HC}$ produced from heavy petroleum films consistently changed over time (absolute-value Spearman's rank correlation coefficient, $\rho_s \geq 0.10$; $p < 0.05$), correlating with 2589 molecular formulas (25.7%), exhibiting a clear separation in van Krevelen space of formula with similar ρ_s values. Two distinct groups were formed. The first (blue) was negatively correlated with time and enriched in aliphatic, unsaturated, low-oxygen, and aromatic compounds (i.e., relatively reduced compounds). The second group (red) was positively correlated with time and enriched with unsaturated, high-oxygen compound classes.[13] The negative and positive correlations with time suggest that the composition of DOM$_{HC}$ produced from the oil films is
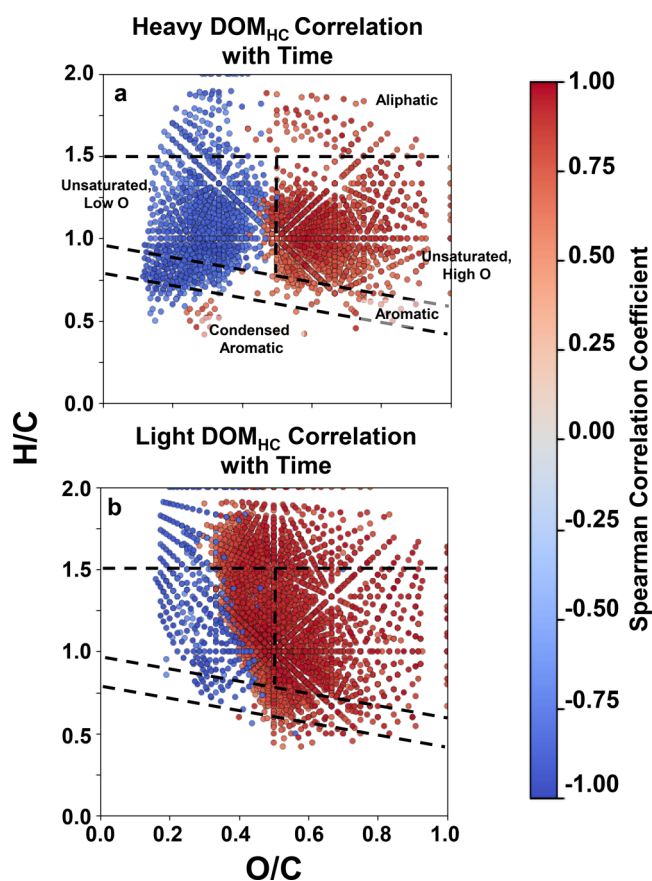
Figure 3. Spearman rank correlations showing relationship between molecular formula derived from FT-ICR MS versus time for DOM$_{HC}$ generated from (a) heavy and (b) light oils.

changing from relatively reduced to oxidized as a function of irradiation time.

The DOM$_{HC}$ produced from light oil also showed a shift in molecular composition over time, as indicated by the increase in the amount of compounds in the red group (absolute-value Spearman's rank correlation coefficient, $\rho_s \geq 0.10$; $p < 0.05$) and correlated with 3541 molecular formulas (34.2%). In comparison to the heavy DOM$_{HC}$, the light DOM$_{HC}$ had fewer aliphatic and unsaturated, low-oxygen compounds negatively correlated with time (blue) and a dramatic increase in aliphatic, unsaturated, low- and high-oxygen, and aromatic compounds that were positively correlated with time (red). The positive correlation with time means that, as more light DOM$_{HC}$ was being produced, the compounds being dissolved into the water became enriched in aliphatic, unsaturated, high-oxygen, and aromatic compounds. In contrast, the heavy DOM$_{HC}$ being produced was mostly highly oxidized material. This distinction observed in the Spearman correlations between these two samples provides strong evidence that the starting composition of the oil plays a major role in the type of compounds that will be photodissolved into the water.

The predominance of more reduced compounds reflected in the shift to low H/C and high O/C after light exposure (Figure 3) coupled to the increase of DOC concentrations over time (Figure 1) both give evidence that the compounds produced in the water from photoirradiation are new compounds and not degradation products of the DOM$_{HC}$ produced at the initial time periods. Furthermore, the oil films were intact (Figure S2 of the Supporting Information) throughout the exposure
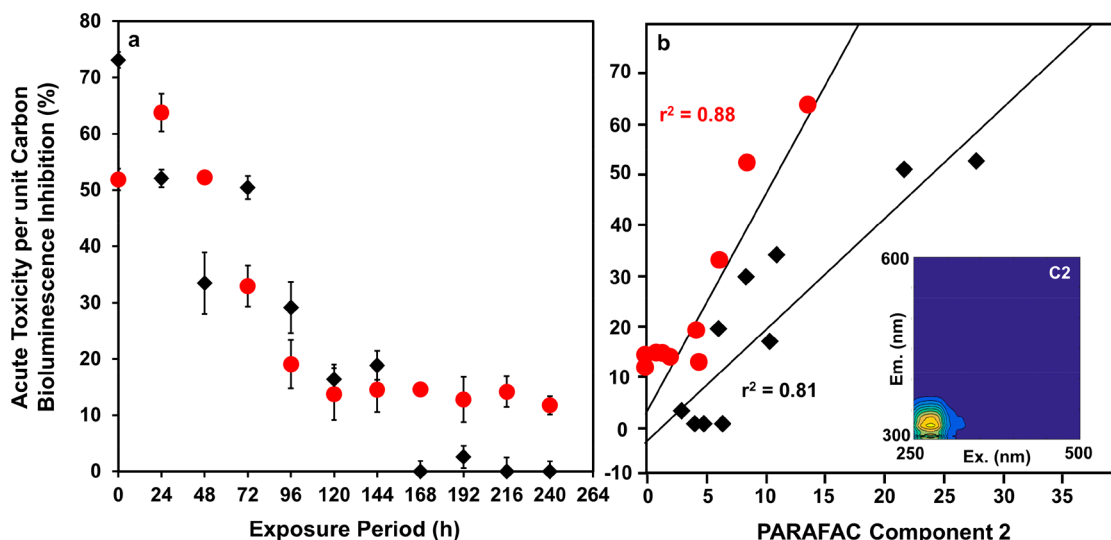
Figure 4. (a) Microtox results for the heavy (black) and light (red) DOM_{HC} for the 15 min incubation period as a function of the exposure period and (b) relationship between PARAFAC component 2 (C2) and acute toxicity per unit carbon.

periods, which shielded the DOM_{HC} from UV exposure, because only the first 10 μm of the oil film absorbs light.[7,48]

3.4. Acute Toxicity Per Unit Carbon of DOM_{HC}. The DOM_{HC} produced from the heavy and light oil films at each exposure period were screened for acute toxicity per unit carbon (% bioluminescence inhibition). We carbon normalized each sample prior to the toxicity screening to assess acute toxicity per unit carbon as a function of the sample composition rather than concentration. Figure 4a presents the carbon-normalized Microtox data and show that, as more DOM_{HC} is produced over time, a decrease in acute toxicity per unit carbon occurs. The maximum acute toxicity per unit carbon for the light DOM_{HC} (62%) and heavy DOM_{HC} (54%) was measured at the initial exposure periods ($T_{24\,h}$), suggesting that the DOM_{HC} produced after the first few hours of simulated sunlight exposure (equivalent to 1 week in the environment) is the most toxic. After 24 h, we observed a rapid decrease in toxicity for both samples, with the heavy DOM_{HC} decreasing with time to 0% and the light DOM_{HC} decreasing from 60 to 20% at 96 h and plateauing to 12% thereafter. These data provide evidence that continual photodissolution of petroleum produces DOM_{HC} and acute toxicity per unit carbon decreases over time. Although a decrease in toxicity per unit carbon over time is observed, the toxicity in the sample (i.e., in the oil spill) may nevertheless increase. Here, the focus was on the relationship between composition and toxicity per unit carbon. Future toxicity measurements will be addressed to understand the overall toxicity as a result of the effect of the concentration.

Relationships between toxicity and optical measurements of DOM_{HC} in previously published work showed that blue-shifted PARAFAC components positively correlated with acute toxicity.[12] To see if any of our components would be a good proxy for acute toxicity per unit carbon, we used OpenFluor[63] to determine if any of our components matched in the database. It was determined that C2 from our model strongly correlated with that which was previously reported at an r^2 value of 0.99, which was also from DOM derived from petroleum.[12,63] Acute toxicity per unit carbon and C2 (Figure 4b) are strongly correlated, suggesting that the toxicity of DOM_{HC} that is produced from photosolubilization of

petroleum can be screened with fluorescence spectroscopy, as suggested by Podgorski et al.[12] Implementing the toxicity index (TI) from Podgorski et al.,[12] we plotted raw fluorescence of peak T/A versus acute toxicity per unit carbon and found a positive correlation ($r^2 = 0.68$) for all of the DOM_{HC} samples (Figure S3 of the Supporting Information). These data show that the TI is an important tool that can be used to screen for toxicity of mobilized water-soluble degradation products where spilled oil is in a water environment.[12]

3.5. Linking the Photoproduction of DOM_{HC} to Optical and Molecular Signatures and Toxicity. PCA was undertaken on all samples (Figure 5) to assess the variables in the DOM_{HC} that correlate optical and molecular composition, toxicity, exposure time, and oil type (heavy oil in red versus light oil in black). PCA 1 accounts for 40% of the
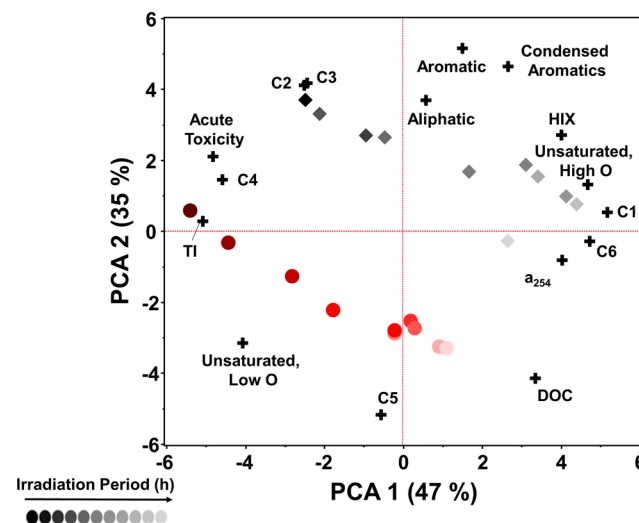
Figure 5. PCA plots showing the relationship of DOM_{HC} generated from heavy oil (black diamonds) and light oil (red circles) as a function of the exposure time (shading decreases with exposure time) for the following data (+): HIX, $SUVA_{254}$, PARAFAC loadings (C1–C6), DOC measurements, percent assigned formulas derived from the FT-ICR MS data, acute toxicity per unit carbon, and TI.

variance in the data. Unsaturated, high-oxygen, aromatic, and condensed aromatic compound classes, DOC, SUVA$_{254}$, and HIX C1 and C6 are positively correlated with PCA 1. Aliphatic and unsaturated, low-oxygen compound classes, PARAFAC components C2, C3, and C4, and acute toxicity per unit carbon correlated negatively with PCA 1. PCA 2 explained 35% of the variance positively correlating with C2, C3, and C4, TI,[12] and acute toxicity per unit carbon and negatively correlating with C5 and aliphatic and unsaturated, low-oxygen compound classes. Over time, the DOM$_{HC}$ composition changed to more aromatic, high-oxygen-containing compounds, with the light DOM$_{HC}$ pooling toward more aromatic-like material (C6, C1, and SUVA$_{254}$) and the heavy DOM$_{HC}$ clustering toward more blue-shifted material with high-oxygen-containing condensed aromatic compounds (C5 and HIX). Acute toxicity per unit carbon strongly clustered with C2, C3, and C4, which were the "oil-derived" fluorescent signatures at the early exposure periods,[62] which provides evidence that the DOM$_{HC}$ produced from the petroleum films in early stages of photooxidation are toxic. Furthermore, there was a clear divide where the heavy DOM$_{HC}$ data points lie in the PCA plot versus the light DOM$_{HC}$, which highlights the different starting compositions of each DOM$_{HC}$ sample. Regardless of the starting composition, both DOM$_{HC}$ samples became more "terrestrial-like" in fluorescence signatures and less toxic over time.

Figure 6 shows a Spearman rank correlation coefficient, where we compared FT-ICR-MS-derived percent assigned
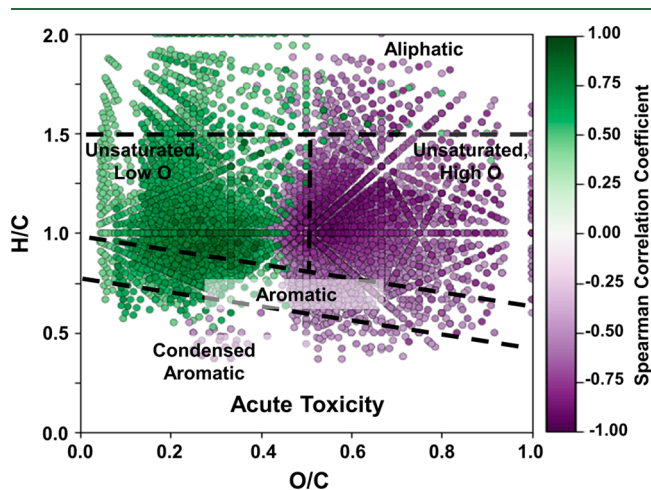
Figure 6. Spearman rank correlations showing the relationship between molecular formula derived from FT-ICR MS versus acute toxicity per unit carbon for DOM$_{HC}$ generated from (a) heavy and (b) light oils. The green dots represent the molecular formula and compound classes correlated with acute toxicity per unit carbon, and the purple dots represent molecular formula and compound classes not correlated with acute toxicity per unit carbon.

classes with acute toxicity per unit carbon across all DOM$_{HC}$ samples. These results show that the reduced compounds (low O/C) are more toxic than the oxidized compounds (high O/C). These data correlate very well with the optical data in that the initial time periods produced the most toxic compounds, but over time, they became less toxic. The changing signatures in the optical and molecular composition as more petroleum-derived carbon is produced into the water provide a wealth of data that allow us to gain insight on the photodissolution of petroleum-derived carbon in water.

The fate of oil spilled in aquatic systems has major impacts on ecosystem health. Exposure to sunlight dramatically changes the composition of petroleum compounds. A strong correlation exists between solar exposure and amount of petroleum-derived carbon solubilized in water, and this dependence varies by the source of the oil. The photo-dissolution of CDOM and comparatively large amounts of non-CDOM will have different degradation pathways in the aqueous phase (i.e., photochemical and microbial processes) that will determine its ultimate fate in aquatic ecosystems. Photodissolution was observed over short and extended time periods (up to 40 days of solar exposure equivalence), indicating that photochemistry plays a role at short times (hours) through much longer time frames. Photochemical transformations result in shifts in optical properties, so that, over time, the fluorescence of transformed-oil-derived molecules resembles that of terrestrial-derived natural organic matter. Such changes mask the signature of oil molecules over time. The bioavailability and acute toxicity per unit carbon of petroleum is also altered by exposure to sunlight. Initially, both are increased because the polarity of these molecules increases as a result of photooxygenation. However, toxicity declines after extended sunlight exposure, suggesting that highly oxygenated photoproducts have decreased toxicity per unit carbon similar to what has been observed for naphthenic acids in oil-sands-produced water.[64] A PARAFAC approach demonstrated that the shifts in toxicity can be followed by simple fluorescence spectroscopy, which can easily be used in field applications. The approaches presented here can provide semi-quantitative data for use in oil spill and damage assessment models and allow for a better understanding of how photochemistry impacts an aquatic oil spill. While additional insight is needed to fully model the fate of spilled oil, this study provides substantial advances that can be applied in actual spill situations. The reactivity and fate of solubilized DOM$_{HC}$ by photochemical and microbial degradation processes are the subject of future studies.

■ ASSOCIATED CONTENT

ⓢ Supporting Information

The Supporting Information is available free of charge on the ACS Publications website at DOI: 10.1021/acs.est.9b01894.

DOC concentrations, a_{254} values, PARAFAC loadings (C1−C5), HIX values, FT-ICR MS data, SUVA$_{254}$, and acute toxicity per unit carbon results for DOM$_{HC}$ produced from light and heavy petroleum (Table S1), FT-ICR MS data versus exposure time for light DOM$_{HC}$ (red) and heavy DOM$_{HC}$ (black) (Figure S1), top view of thin oil films after prolonged irradiation for heavy oil (left) and light oil (right) in thermostatically controlled jacketed beakers (Figure S2), and TI of raw fluorescence of peaks T and A versus percent acute toxicity per unit carbon (Figure S3) (PDF)

■ AUTHOR INFORMATION

Corresponding Author

*E-mail: pazito@uno.edu.

ORCID ⓞ

Phoebe Zito: 0000-0002-7011-1940

David C. Podgorski: 0000-0002-1070-5923

Ryan P. Rodgers: 0000-0003-1302-2850

Matthew A. Tarr: 0000-0002-3399-1336

Present Address

‖Joshua Johnson: Department of Chemistry, Purdue University, 560 Oval Drive, West Lafayette, Indiana 47907-2084, United States.

Notes

The authors declare no competing financial interest.

■ ACKNOWLEDGMENTS

■ REFERENCES

(1) Aeppli, C.; Carmichael, C.; Nelson, R. K.; Lemkau, K. L.; Graham, W. M.; Redmond, M. C.; Valentine, D. L.; Reddy, C. M. Oil Weathering after the Deepwater Horizon Disaster Led to the Formation of Oxygenated Residues. *Environ. Sci. Technol.* **2012**, *46*, 8799−8807.

(2) Ryerson, T. B.; Camilli, R.; Kessler, J. D.; Kujawinski, E. B.; Reddy, C. M.; Valentine, D. L.; Atlas, E.; Blake, D. R.; de Gouw, J.; Meinardi, S.; Parrish, D. D.; Peischl, J.; Seewald, J. S.; Warneke, C. Chemical data quantify Deepwater Horizon hydrocarbon flow rate and environmental distribution. *Proc. Natl. Acad. Sci. U. S. A.* **2012**, *109* (50), 20246−20253.

(3) Reddy, C. M.; Arey, J. S.; Seewald, J. S.; Sylva, S. P.; Lemkau, K. L.; Nelson, R. K.; Carmichael, C. A.; McIntyre, C. P.; Fenwick, J.; Ventura, G. T.; Van Mooy, B. A. S.; Camilli, R. Composition and fate of gas and oil released to the water column during the Deepwater Horizon oil spill. *Proc. Natl. Acad. Sci. U. S. A.* **2012**, *109* (50), 20229−20234.

(4) Wilson, M.; Graham, L.; Hale, C.; Maung-Douglass, E.; Sempier, S.; Skelton, T.; Swann, L. *Oil Spill Science: Deepwater Horizon—Where Did the Oil Go*; Sea Grant: Silver Spring, MD, 2017; GOMSG-G-17-006.

(5) Jordan, R. E.; Payne, J. R. *Fate and Weathering of Petroleum Spills in the Marine Environment: A Literature Review and Synopsis*; Ann Arbor Science Publishers, Inc.: Ann Arbor, MI, 1980.

(6) Tarr, M. A.; Zito, P.; Overton, E. B.; Olson, G. M.; Adkikari, P. L.; Reddy, C. M. Weathering of Oil Spilled in the Marine Environment. *Oceanography* **2016**, *29* (3), 126−135.

(7) Ward, C. P.; Sharpless, C. M.; Valentine, D. L.; French-McCay, D. P.; Aeppli, C.; White, H. K.; Rodgers, R. P.; Gosselin, K. M.; Nelson, R. K.; Reddy, C. M. Partial Photochemical Oxidation Was a Dominant Fate of Deepwater Horizon Surface Oil. *Environ. Sci. Technol.* **2018**, *52* (4), 1797−1805.

(8) Aeppli, C.; Nelson, R. K.; Carmichael, C. A.; Arakawa, N.; Aluwihare, L. I.; Valentine, D. L.; Reddy, C. M. Characterization of Recalcitrant Oxygenated Hydrocarbons Formed upon Oil Weathering after the Deepwater Horizon Disaster. *Proceedings of the 245th ACS National Meeting & Exposition*; New Orleans, LA, April 7−11, 2013; Abstract 150-GEOC.

(9) Harriman, B. H.; Zito, P.; Podgorski, D. C.; Tarr, M. A.; Suflita, J. M. Impact of Photooxidation and Biodegradation on the Fate of Oil Spilled During the Deepwater Horizon Incident: Advanced Stages of Weathering. *Environ. Sci. Technol.* **2017**, *51* (13), 7412−7421.

(10) Bianchi, T. S.; Osburn, C.; Shields, M. R.; Yvon-Lewis, S.; Young, J.; Guo, L.; Zhou, Z. Deepwater Horizon Oil in Gulf of Mexico Waters after 2 Years: Transformation into the Dissolved Organic Matter Pool. *Environ. Sci. Technol.* **2014**, *48* (16), 9288−9297.

(11) Thorn, K. A.; Aiken, G. R. Biodegradation of crude oil into nonvolatile organic acids in a contaminated aquifer near Bemidji, Minnesota. *Org. Geochem.* **1998**, *29* (4), 909−931.

(12) Podgorski, D. C.; Zito, P.; McGuire, J. T.; Martinovic-Weigelt, D.; Cozzarelli, I. M.; Bekins, B. A.; Spencer, R. G. M. Examining Natural Attenuation and Acute Toxicity of Petroleum-Derived Dissolved Organic Matter with Optical Spectroscopy. *Environ. Sci. Technol.* **2018**, *52* (11), 6157−6166.

(13) Ray, P. Z.; Chen, H.; Podgorski, D. C.; McKenna, A. M.; Tarr, M. A. Sunlight creates oxygenated species in water-soluble fractions of Deepwater horizon oil. *J. Hazard. Mater.* **2014**, *280*, 636−643.

(14) Larson, R. A.; Hunt, L. L.; Blankenship, D. W. Formation of Toxic Products from a #2 Fuel Oil by Photooxidation. *Environ. Sci. Technol.* **1977**, *11* (5), 492−496.

(15) Zhou, Z.; Liu, Z.; Guo, L. Chemical evolution of Macondo crude oil during laboratory degradation as characterized by fluorescence EEMs and hydrocarbon composition. *Mar. Pollut. Bull.* **2013**, *66* (1), 164−175.

(16) Fay, J. A. Physical Processes in the spread of oil on a water surface. *International Oil Spill Conference Proceedings* **1971**, *1971*, 463−467.

(17) Alan Roebuck, J.; Podgorksi, D. C.; Wagner, S.; Jaffé, R. Photodissolution of charcoal and fire-impacted soil as a potential source of dissolved black carbon in aquatic environments. *Org. Geochem.* **2017**, *112*, 16−21.

(18) Stubbins, A.; Spencer, R. G. M.; Chen, H.; Hatcher, P. G.; Mopper, K.; Hernes, P. J.; Mwamba, V. L.; Mangangu, A. M.; Wabakanghanzi, J. N.; Six, J. Illuminated darkness: Molecular signatures of Congo River dissolved organic matter and its photochemical alteration as revealed by ultrahigh precision mass spectrometry. *Limnol. Oceanogr.* **2010**, *55* (4), 1467−1477.

(19) King, S.; Leaf, P.; Olson, A.; Ray, P.; Tarr, M. Photolytic and photocatalytic degradation of surface oil from the Deepwater Horizon spill. *Chemosphere* **2014**, *95*, 415−422.

(20) Ohno, T. Fluorescence inner-filtering correction for determining the humification index of dissolved organic matter. *Environ. Sci. Technol.* **2002**, *36*, 742−746.

(21) Kowalczuk, P.; Cooper, W. J.; Whitehead, R. F.; Durako, M. J.; Sheldon, W. Characterization of CDOM in an organic-rich river and surrounding coastal ocean in the South Atlantic Bight. *Aquat. Sci.* **2003**, *65* (4), 384−401.

(22) Stedmon, C. A.; Bro, R. Characterizing dissolved organic matter fluorescence with parallel factor analysis: A tutorial. *Limnol. Oceanogr.: Methods* **2008**, *6*, 572−579.

(23) Spencer, R. G. M.; Bolton, L.; Baker, A. Freeze/thaw and pH effects on freshwater dissolved organic matter fluorescence and absorbance properties from a number of UK locations. *Water Res.* **2007**, *41*, 2941−2950.

(24) Yan, M.; Fu, Q.; Li, D.; Gao, G.; Wang, D. Study of the pH influence on the optical properties of dissolved organic matter using fluorescence excitation-emission matrix and parallel factor analysis. *J. Lumin.* **2013**, *142*, 103−109.

(25) Tfaily, M. M.; Podgorski, D. C.; Corbett, J. E.; Chanton, J. P.; Cooper, W. T. Influence of acidification on the optical properties and molecular composition of dissolved organic matter. *Anal. Chim. Acta* **2011**, *706*, 261−267.

(26) Weishaar, J. L.; Aiken, G. R.; Bergamaschi, B. A.; Fram, M. S.; Fujii, R.; Mopper, K. Evaluation of Specific Ultraviolet Absorbance as an Indicator of the Chemical Composition and Reactivity of Dissolved Organic Carbon. *Environ. Sci. Technol.* **2003**, *37* (20), 4702−4708.

(27) Kaiser, K. L. E. Correlations of *Vibrio fischeri* bacteria test data with bioassay data for other organisms. *Environ. Health Perspect.* **1998**, *106* (Supplement 2), 583−591.

(28) Dewhurst, R. E.; Wheeler, J. R.; Chummun, K. S.; Mather, J. D.; Callaghan, A.; Crane, M. The comparison of rapid bioassays for the assessment of urban groundwater quality. *Chemosphere* **2002**, *47* (5), 547−554.

(29) Dittmar, T.; Koch, B.; Hertkorn, N.; Kattner, G. A simple and efficient method for the solid-phase extraction of dissolved organic matter (SPE-DOM) from seawater. *Limnol. Oceanogr.: Methods* **2008**, *6* (6), 230−235.

(30) Blakney, G. T.; Hendrickson, C. L.; Marshall, A. G. Predator data station: A fast data acquisition system for advanced FT-ICR MS experiments. *Int. J. Mass Spectrom.* **2011**, *306* (2−3), 246−252.

(31) Kaiser, N. K.; Quinn, J. P.; Blakney, G. T.; Hendrickson, C. L.; Marshall, A. G. A Novel 9.4 T FTICR Mass Spectrometer with Improved Sensitivity, Mass Resolution, and Mass Range. *J. Am. Soc. Mass Spectrom.* **2011**, *22* (8), 1343−1351.

(32) Kaiser, N. K.; Quinn, J. P.; Blakney, G. T.; Hendrickson, C. L.; Marshall, A. G. A novel 9.4 T FTICR mass spectrometer with improved sensitivity, mass resolution, and mass range. *J. Am. Soc. Mass Spectrom.* **2011**, *22* (8), 1343−1351.

(33) Corilo, Y. *EnviroOrg*; Florida State University: Tallahassee, FL, 2015.

(34) Savory, J. J.; Kaiser, N. K.; McKenna, A. M.; Xian, F.; Blakney, G. T.; Rodgers, R. P.; Hendrickson, C. L.; Marshall, A. G. Parts-Per-Billion Fourier Transform Ion Cyclotron Resonance Mass Measurement Accuracy with a "Walking" Calibration Equation. *Anal. Chem.* **2011**, *83* (5), 1732−1736.

(35) Koch, B. P.; Dittmar, T. From Mass to Structure: An Aromaticity Index for High-Resolution Mass Data of Natural Organic Matter. *Rapid Commun. Mass Spectrom.* **2006**, *20*, 926−932.

(36) Šantl-Temkiv, T.; Finster, K.; Dittmar, T.; Hansen, B. M.; Thyrhaug, R.; Nielsen, N. W.; Karlson, U. G. Hailstones: A Window into the Microbial and Chemical Inventory of a Storm Cloud. *PLoS One* **2013**, *8* (1), e53550.

(37) Spencer, R. G. M.; Guo, W.; Raymond, P. A.; Dittmar, T.; Hood, E.; Fellman, J.; Stubbins, A. Source and biolability of ancient dissolved organic matter in glacier and lake ecosystems on the Tibetan Plateau. *Geochim. Cosmochim. Acta* **2014**, *142*, 64−74.

(38) Hemingway, J. D. *Fouriertransform: Open-Source Tools for FT-ICR MS Data Analysis*, 2017; https://github.com/FluvialSeds/fouriertransform.

(39) Murphy, K. R.; Stedmon, C. A.; Graeber, D.; Bro, R. Fluorescence spectroscopy and multi-way techniques. PARAFAC. *Anal. Methods* **2013**, *5* (23), 6557.

(40) Helms, J. R.; Stubbins, A.; Perdue, E. M.; Green, N. W.; Chen, H.; Mopper, K. Photochemical bleaching of oceanic dissolved organic matter and its effect on absorption spectral slope and fluorescence. *Mar. Chem.* **2013**, *155*, 81−91.

(41) Zonneveld, K. A. F.; Versteegh, G. J. M.; Kasten, S.; Eglinton, T. I.; Emeis, K.-C.; Huguet, C.; Koch, B. P.; de Lange, G. J.; de Leeuw, J. W.; Middelburg, J. J.; Mollenhauer, G.; Prahl, F. G.; Rethemeyer, J.; Wakeham, S. G. Selective preservation of organic matter in marine environments; processes and impact on the sedimentary record. *Biogeosciences* **2010**, *7*, 483−511.

(42) Lemkau, K. L.; Peacock, E. E.; Nelson, R. K.; Ventura, G. T.; Kovecses, J. L.; Reddy, C. M. The M/V Cosco Busan spill: Source identification and short-term fate. *Mar. Pollut. Bull.* **2010**, *60* (11), 2123−2129.

(43) Coble, P. G. Marine Optical Biogeochemistry: The Chemistry of Ocean Color. *Chem. Rev.* **2007**, *107* (2), 402−418.

(44) Yamashita, Y.; Boyer, J. N.; Jaffé, R. Evaluating the distribution of terrestrial dissolved organic matter in a complex coastal ecosystem using fluorescence spectroscopy. *Cont. Shelf Res.* **2013**, *66*, 136−144.

(45) Kowalczuk, P.; Tilstone, G. H.; Zabłocka, M.; Röttgers, R.; Thomas, R. Composition of dissolved organic matter along an Atlantic Meridional Transect from fluorescence spectroscopy and Parallel Factor Analysis. *Mar. Chem.* **2013**, *157*, 170−184.

(46) McKnight, D. M.; Boyer, E. W.; Westerhoff, P. K.; Doran, P. T.; Kulbe, T.; Andersen, D. T. Spectrofluorometric characterization of dissolved organic matter for indication of precursor organic material and aromaticity. *Limnol. Oceanogr.* **2001**, *46* (1), 38−48.

(47) Stedmon, C. A.; Markager, S. Behaviour of the optical properties of coloured dissolved organic matter under conservative mixing. *Estuarine, Coastal Shelf Sci.* **2003**, *57* (5), 973−979.

(48) Ray, P. Z.; Tarr, M. A. Solar Production of Singlet Oxygen from Crude Oil Films on Water. *J. Photochem. Photobiol., A* **2014**, *286*, 22−28.

(49) Ray, P.; Tarr, M. Petroleum films exposed to sunlight produce hydroxyl radical. *Chemosphere* **2014**, *103*, 220−227.

(50) Ray, P. Z.; Tarr, M. A. Formation of organic triplets from solar irradiation of petroleum. *Mar. Chem.* **2015**, *168*, 135−139.

(51) Ishida, H.; Takahashi, H.; Sato, H.; Tsubomura, H. Interaction of oxygen with organic molecules. I. Absorption spectra caused by adsorbed organic molecules and oxygen. *J. Am. Chem. Soc.* **1970**, *92* (2), 275−280.

(52) Evans, D. F. Magnetic Perturbation of the Lowest Triplet States of Aromatic Molecules by Dissolved Oxygen. *Nature* **1956**, *178*, 534.

(53) Graeber, D.; Gelbrecht, J.; Pusch, M. T.; Anlanger, C.; von Schiller, D. Agriculture has changed the amount and composition of dissolved organic matter in Central European headwater streams. *Sci. Total Environ.* **2012**, *438*, 435−446.

(54) Murphy, K. R.; Ruiz, G. M.; Dunsmuir, W. T. M.; Waite, T. D. Optimized Parameters for Fluorescence-Based Verification of Ballast Water Exchange by Ships. *Environ. Sci. Technol.* **2006**, *40* (7), 2357−2362.

(55) Yamashita, Y.; Kloeppel, B. D.; Knoepp, J.; Zausen, G. L.; Jaffé, R. Effects of Watershed History on Dissolved Organic Matter Characteristics in Headwater Streams. *Ecosystems* **2011**, *14* (7), 1110−1122.

(56) Walker, S. A.; Amon, R. M. W.; Stedmon, C.; Duan, S.; Louchouarn, P. The use of PARAFAC modeling to trace terrestrial dissolved organic matter and fingerprint water masses in coastal Canadian Arctic surface waters. *J. Geophys. Res.: Biogeosci.* **2009**, *114* (G4), G00F06.

(57) Gonnelli, M.; Galletti, Y.; Marchetti, E.; Mercadante, L.; Retelletti Brogi, S.; Ribotti, A.; Sorgente, R.; Vestri, S.; Santinelli, C. Dissolved organic matter dynamics in surface waters affected by oil spill pollution: Results from the Serious Game exercise. *Deep Sea Res., Part II* **2016**, *133*, 88−99.

(58) Murphy, K. R.; Hambly, A.; Singh, S.; Henderson, R. K.; Baker, A.; Stuetz, R.; Khan, S. J. Organic Matter Fluorescence in Municipal Water Recycling Schemes: Toward a Unified PARAFAC Model. *Environ. Sci. Technol.* **2011**, *45* (7), 2909−2916.

(59) Osburn, C.; Stedmon, C. A. Linking the chemical and optical properties of dissolved organic matter in the Baltic−North Sea transition zone to differentiate three allochthonous inputs. *Mar. Chem.* **2011**, *126*, 281−294.

(60) Coble, P. G. Characterization of marine and terrestrial DOM in seawater using excitation-emission matrix spectroscopy. *Mar. Chem.* **1996**, *51*, 325−346.

(61) Zhou, Z.; Guo, L. Evolution of the optical properties of seawater influenced by the Deepwater Horizon oil spill in the Gulf of Mexico. *Environ. Res. Lett.* **2012**, *7* (2), 025301.

(62) Zhou, Z.; Guo, L.; Shiller, A. M.; Lohrenz, S. E.; Asper, V. L.; Osburn, C. L. Characterization of oil components from the Deepwater Horizon oil spill in the Gulf of Mexico using fluorescence EEM and PARAFAC techniques. *Mar. Chem.* **2013**, *148*, 10−21.

(63) Murphy, K. R.; Stedmon, C. A.; Wenig, P.; Bro, R. OpenFluor—An online spectral library of auto-fluorescence by organic compounds in the environment. *Anal. Methods* **2014**, *6* (3), 658−661.

(64) Headley, J. V.; McMartin, D. W. A Review of the Occurrence and Fate of Naphthenic Acids in Aquatic. *J. Environ. Sci. Health, Part A: Toxic/Hazard. Subst. Environ. Eng.* **2004**, *39* (8), 1989−2010.